1 **Title: Rapid detection of DNA and RNA shrimp viruses using CRISPR-based diagnostics**

2 Running title: CRISPR diagnostics detect DNA and RNA shrimp viruses

3 Samuel R. Major[a], Matthew J. Harke[a], Roberto Cruz-Flores[b*], Arun K. Dhar[b], Andrea G.

4 Bodnar[a], and Shelly A. Trigg[a#]

5

6 [a]Gloucester Marine Genomics Institute, Gloucester, MA, United States.

7 [b]Aquaculture Pathology Laboratory, School of Animal and Comparative Biomedical Sciences,

8 The University of Arizona, Tucson, AZ, United States.

9 [*]Centro de Investigación Científica y de Educación Superior de Ensenada, (CICESE), Carretera

10 Ensenada-Tijuana No. 3918, Zona Playitas, 22860 Ensenada, Baja California, Mexico.

11 [#]Please address manuscript correspondence to Shelly A. Trigg (shelly.trigg@gmgi.org).

12 Abstract word count: 238

13 Main text word count: 4739

14

15 **ABSTRACT**

16 Timely detection of persistent and emerging pathogens is critical to controlling disease
17 spread, particularly in high-density populations with increased contact between individuals and
18 limited-to-no ability to quarantine. Standard molecular diagnostic tests for surveying pathogenic
19 microbes have provided the sensitivity needed for early detection, but lag in time-to-result
20 leading to delayed action. On-site diagnostics alleviate this lag, but current technologies are less
21 sensitive and adaptable than lab-based molecular methods. Towards the development of
22 improved on-site diagnostics, we demonstrated the adaptability of a loop-mediated isothermal
23 amplification-CRISPR coupled technology for detecting DNA and RNA viruses that have
24 greatly impacted shrimp populations worldwide; White Spot Syndrome Virus and Taura
25 Syndrome Virus. Both CRISPR-based fluorescent assays we developed showed similar
26 sensitivity and accuracy for viral detection and load quantification to real-time PCR.
27 Additionally, both assays specifically targeted their respective virus with no false positives
28 detected in animals infected with other common pathogens or in certified specific pathogen-free
29 animals.

30 **IMPORTANCE**

31 The Pacific white shrimp (*Penaeus vannamei*) is one of the most valuable aquaculture
32 species in the world, but has suffered major economic losses from outbreaks of White Spot
33 Syndrome Virus and Taura Syndrome Virus. Rapid detection of these viruses can improve
34 aquaculture practices by enabling more timely action to be taken to combat disease outbreaks.
35 Highly sensitive, specific, and robust CRISPR-based diagnostic assays such as those developed
36 here have the potential to revolutionize disease management in agriculture and aquaculture
37 helping to promote global food security.

38 **INTRODUCTION**

39 The ability to rapidly detect disease is a major challenge not just in human health but
40 across all farmed and wild animal health monitoring. While methods for disease detection have
41 advanced the field of molecular diagnostics to the global role it plays today, limitations posed by
42 laboratory-based technologies hinder the ability to quickly respond to disease outbreaks. For
43 example, culturing and molecular diagnostics using PCR-based methods provide the high
44 sensitivity needed for early pathogen detection, but they require laboratory processing (e.g.
45 sophisticated equipment, expensive reagents, and specialized training) leading to long turnaround
46 times for results (several days) and delayed action for disease mitigation. Contrastingly,
47 immunochromatographic antigen diagnostics are field-deployable, affordable and provide rapid
48 results, but comparatively lack sensitivity and require more time for assay creation resulting in a
49 longer time to respond to emerging pathogens. Alternative molecular diagnostics that require less
50 sophisticated equipment like loop-mediated isothermal amplification (LAMP) have recently been
51 developed, but their superior amplification efficiency can stochastically yield false positive
52 results (1). In human health, CRISPR-based molecular diagnostics, such as the SHERLOCK
53 (Specific High sensitivity Enzymatic Reporter UnLOCKing) technology, have emerged to
54 overcome the limitations of PCR and antigen tests to enable rapid, sensitive, inexpensive, and
55 accurate on-site detection of viruses and other pathogens (2). SHERLOCK combines the
56 efficiency of isothermal amplification with the specificity of CRISPR detection for highly
57 sensitive, specific and robust diagnostics that can be used in low resource settings (3). A second-
58 generation SHERLOCK assay that uses a heat tolerant Cas enzyme, Cas12b, coupled with
59 LAMP showed highly sensitive, rapid, and robust detection of viral RNA from SARS-CoV-2 (4).

60 Applications beyond human health in veterinary pathology and disease diagnostics in agriculture
61 and aquaculture settings could have a tremendous impact on domestic and global food security.

62 Aquaculture is the fastest growing animal protein production sector globally, with
63 production expected to double by 2050 to meet the demand of the growing population (5, 6).
64 However, production is greatly impeded by infectious diseases highlighting the urgent need for
65 rapid, sensitive, and accurate diagnostics. For example, Pacific white shrimp (*Penaeus*
66 *vannamei*) production, that accounts for ~25% of all seafood products consumed annually, has
67 suffered major economic losses due to infections caused by viruses like White Spot Syndrome
68 Virus (WSSV) and Taura Syndrome Virus (TSV) (7–9). These diseases have resulted in up to
69 100% mortality in as few as seven days (10, 11). The DNA virus WSSV has been the leading
70 cause of economic losses in shrimp aquaculture globally since its emergence in 1991, costing
71 ~$1 billion and reducing global shrimp production by ~10% annually (7). TSV, a single stranded
72 RNA virus, has caused mass mortality events on at least five continents since its emergence in
73 1991, with an estimated total loss of $2 billion from 1992-1996 (12–14). Although Taura
74 syndrome caused by TSV is no longer causing economic losses to the extent it has in the past,
75 with the current availability and farming of TSV-tolerant shrimp lines (15), WSSV-tolerant
76 shrimp are still under development and are not commercially available (16). The domestic
77 development and international import of specific pathogen-free (SPF) shrimp stocks has
78 mitigated some disease outbreaks. However, even with routine rigorous screening disease
79 continues to be a major threat. For instance, shrimp stocks in Brazil and Colombia were reported
80 to be contaminated from imported SPF shrimp with underlying TSV infection that went
81 undetected (17). The more recently documented spread of WSSV in Australia, India, and
82 Ecuador has resulted in the virus being labeled as the most devasting pathogen in the

83 aquacultural history of shrimp farming (18–20). To ensure globally distributed stocks are
84 disease-free and to mitigate production losses for improved food security, it is crucial that rapid,
85 accurate, and sensitive diagnostics are available to shrimp farmers (21, 22).

86 To mitigate losses due to viral diseases in shrimp aquaculture, we recently developed a
87 CRISPR-based SHERLOCK diagnostic assay (SHERLOCKv1) that can detect WSSV in shrimp
88 tissue (23). Building upon this success, and incorporating second generation SHERLOCK
89 technology, we demonstrate the adaptability of this technology for both DNA and RNA viral
90 targets and present two second-generation SHERLOCK (SHERLOCKv2) assays that detect
91 WSSV and TSV. These robust, sensitive, and specific lab-based fluorescent assays can detect
92 viral target in shrimp tissue in under one hour. They also enable field-deployable conversion for
93 improved diagnostic capabilities of viral outbreaks in aquaculture settings. This demonstration of
94 assay adaptation for diverse shrimp diseases paves the way for next generation assay
95 development in veterinary pathology and animal diagnostics for improved disease management
96 in aquaculture and agriculture.

97 **RESULTS**

98 *Diagnostic assay development*

99 Combining the robustness of LAMP with the specificity of CRISPR and detection of
100 Cas12b collateral cleavage activity, we developed sensitive and specific one-pot SHERLOCKv2
101 assays for the detection of DNA and RNA viruses that negatively impact shrimp aquaculture
102 worldwide; WSSV and TSV (**Figure 1**). In an initial screen to identify an optimal LAMP primer
103 set targeting a conserved TSV genome region, we compared the amplification activity of three
104 primer sets as well as a previously published LAMP primer set (24). We found the previously
105 published set targeting the capsid protein gene between VP1 and VP3 domains showed the

106 fastest, most sensitive detection of TSV and selected this set for the SHERLOCKv2 assay
107 (**Figure S1a-b**). In designing the WSSV assay, the highly conserved viral protein 28 (VP28) was
108 targeted to limit the ability of WSSV strain to influence detection. Of the four LAMP primer sets
109 designed and screened, one set (VP28.31) showed superior speed (**Figure S1c-d**). The addition
110 of poly-T linkers between the two annealing sites within the FIP and BIP primers increased both
111 the speed and sensitivity of the primer set down to 100 copies (**Figure S1e**).
112 Of the 12 guide RNAs designed to target within the TSV LAMP target region, one guide
113 RNA (cr9225) produced cleavage signals before 30 minutes with low variance among replicate
114 reactions and minimal background signal, and was selected for the TSV SHERLOCKv2 assay
115 (**Figure S2a-b**). Of the 11 guide RNAs designed to target within the WSSV LAMP target region,
116 one guide RNA (VP28_27) showed the highest cleavage signal with the greatest signal-to-
117 background ratio and was selected for the WSSV SHERLOCKv2 assay (**Figure S2c-d**).
118 Furthermore, we found that the addition of glycine, a reaction temperature of 62°C, 2 µM
119 reporter concentration, and a guide RNA-to-Cas12b ratio of 1:1 consistently gave optimal signal-
120 to-background in the WSSV SHERLOCKv2 assay. Because the addition of carrier nucleic acid
121 has shown improvements to sensitivity and specificity in RT-LAMP reactions (25), we tested
122 this in the TSV SHERLOCKv2 assay and found that the addition of 5 or 10 ng of non-target
123 carrier RNA produced the highest signal with the least variance among replicates (**Figure S3a**).
124 For WSSV SHERLOCKv2 assay, we decided to use 20 ng of non-target carrier DNA because
125 that was the upper limit of input material reported in the WSSV SHERLOCKv1 limit-of-
126 detection experiment and this amount would allow input for subsequent experiments to be
127 standardized.
128 *Assay sensitivity and specificity*

129 To evaluate assay sensitivity, we generated standard curves using 10-fold dilutions of the
130 synthetic TSV target RNA, WSSV target DNA, or genomic DNA isolated from WSSV-infected
131 shrimp. Both assays consistently detected down to 100 copies with a strong correlation to the
132 amount of nucleic acid input (**Figure 2a-b and S4**). In comparing dilution series from 19
133 independent experiments, we found synthetic target to be comparable to genomic target isolated
134 from shrimp with high TSV and WSSV viral loads previously quantified by qPCR, confirming
135 that synthetic target can be used for estimating TSV and WSSV copy number quantity in
136 genomic samples (**Figure S4**). In experiments evaluating assay specificity, both SHERLOCKv2
137 assays showed high specificity for their target pathogen. Only TSV-infected and WSSV-infected
138 shrimp samples showed Cas12b collateral cleavage signal compared to samples from shrimp
139 infected with other common shrimp pathogens (IMNV, IHHNV, EHP and *Vibrio*
140 *parahaemolyticus* causing AHPND/EMS) (**Figure 2c-d**). Furthermore, both assays showed no
141 false positive detection in samples from specific pathogen-free shrimp (**Figure 2c-d)**. While we
142 did observe stochastic non-specific LAMP signal in some true negative samples, this did not lead
143 to Cas cleavage and did not result in positive viral detection (**Figure S5**).
144 *Assay validaiton*
145 To estimate the diagnostic sensitivity of the SHERLOCKv2 assays, we tested shrimp
146 samples from different TSV and WSSV challenge experiments in SHERLOCKv2 assays and in
147 the OIE (World Organization for Animal Health) recommended real-time PCR diagnostic for
148 TSV and WSSV (26). Assays were run alongside standard curves to quantify and compare viral
149 copy number determined by each method (real-time PCR hereinafter referred to as qPCR). In the
150 TSV challenge experiments, because most commercially available genetic lines of shrimp being
151 tolerant to TSV, two different commercial lines of *P. vannamei* known to differ in their

152 susceptibility and two different TSV isolates known to differ in their virulence were used. The
153 Belize isolate used to infect the TSV-tolerant *P. vannamei* line is known to be highly virulent
154 and has led to TSV infection in TSV-tolerant commercial *P. vannamei* lines, where the TSV-
155 susceptible Kona line has shown high rates of infection regardless of the TSV isolate used in
156 challenge experiments (27). Following the challenge experiments, the TSV-susceptible line
157 showed pathognomonic lesions of TSV characterized by necrosis, pyknosis, and karyorrhexis of
158 the cuticular epithelium within the appendages, gills, and exocuticle (**Figure 3a**). In addition,
159 some of these showed mortalities during the course of the experiment. However, the TSV-
160 tolerant *P. vannamei* showed no TSV-associated pathognomonic lesions or mortalities (**Figure**
161 **3b**). Because of the wide dynamic range in viral load expected in these samples, we did a
162 titration experiment to determine an optimal amount of sample input for TSV detection with the
163 TSV SHERLOCK assay. We determined that 10 ng of TSV-infected shrimp genomic DNA led
164 to the least variable and highest signal (**Figure S3b**), and this amount was used for subsequent
165 TSV SHERLOCKv2 and qPCR experiments. The qPCR detected TSV in all TSV-challenged
166 shrimp samples (**Figures 3c**, **Table S3**). The TSV SHERLOCK assay detected TSV in 26 out of
167 the 30 TSV-challenged shrimp samples (87% positive percent agreement) (**Table S3**). The four
168 samples for which SHERLOCK did not detect TSV had low viral load extrapolated from a
169 standard curve (three had < 1000 copies and one had ~5000 copies). Both qPCR or SHERLOCK
170 TSV assays showed a significant effect of challenge experiment on the viral load (Mann-
171 Whitney-U test $P = 0.006395$ and $P = 0.003415$, respectively). Viral copy concentration
172 predicted by SHERLOCK showed a statistically significant correlation with that predicted by
173 qPCR ($R = 0.93$, $p = 1.5\times10^{-11}$; **Figure 3d**) with SHERLOCK tending to underestimate viral
174 copies relative to qPCR (**Figure 4a**).

175 For WSSV, we tested the same WSSV-infected *P. vannamei* samples previously
176 quantified by the OIE-recommended WSSV qPCR and the SHERLOCKv1 assay (23). Given
177 that these samples previously showed high viral loads and material was limited, 1 ng of WSSV-
178 infected shrimp genomic DNA was used in each SHERLOCKv2 reaction. Of the 35 WSSV-
179 infected *P. vannamei* samples tested alongside standard curves, we detected infection in 33
180 samples (94% positive percent agreement) (**Table S3**). The two samples where no WSSV was
181 detected were expected to have low viral copies based on qPCR estimations (~40 copies and 800
182 copies). Moreover, viral copy concentrations measured by WSSV SHERLOCKv2 were mostly
183 similar to those quantified by qPCR (**Figure 4a**). Compared to the previous version WSSV
184 SHERLOCKv1 assay that used RPA and Cas13a enzymes (23), SHERLOCKv2 showed less
185 variation across technical replicates than SHERLOCKv1 (**Figure 4b**). There was a statistically
186 significant correlation between SHERLOCKv2 and qPCR viral copy quantifications (R = 0.79, P
187 = 9.8×10^{-8}), and between SHERLOCKv2 and SHERLOCKv1 viral copy quantifications (R =
188 0.75, $P = 9.6\times10^{-7}$) (**Figure 5**).
189

190 **DISCUSSION**

191 With the goal of adapting cutting-edge human diagnostic technology to diseases
192 impacting food security, we developed two different rapid and highly specific lab-based one-pot
193 SHERLOCK fluorescent assays for the detection of common shrimp pathogens. We demonstrate
194 the adaptability of the SHERLOCK platform for targeting either a common RNA virus (TSV) or
195 a common DNA virus (WSSV) that have impacted shrimp aquaculture globally. We found the
196 TSV and WSSV SHERLOCKv2 assays to have a sensitivity and quantitative capability on par
197 with the OIE-recommended qPCR assays for these diseases. Moreover, both assays can assess
198 infection status for a variety of samples in as little as 30 minutes, improving upon the time-to-

199 result of qPCR. With the demonstrated ease of converting a one-pot fluorescent SHERLOCK
200 assay to a field-deployable assay (3, 23), these assays lay the foundation for rapid, specific field
201 diagnostics in shrimp aquaculture.

202 Building on an earlier iteration of a WSSV SHERLOCK assay, we were able to simplify
203 assay components leading to more robust and repeatable detection of both DNA and RNA viral
204 targets. The previous WSSV SHRELOCK assay used recombinase polymerase amplification
205 (RPA) to amplify DNA target, RNA polymerase to convert the amplified target from DNA to
206 RNA, and Cas13a to detect RNA target (23). The SHERLOCKv2 assays presented in this study
207 use LAMP (with or without reverse transcriptase) and Cas12b to detect DNA target from RNA
208 or DNA input, following the successful SARS-CoV-2 SHERLOCK assay design (4). By
209 eliminating the need for converting input material to RNA and relying on Cas13a for RNA
210 detection, these SHERLOCKv2 assays enable more stable and robust target detection. This is
211 supported by the reduced variation across technical replicates observed for WSSV
212 SHERLOCKv2 compared to WSSV SHERLOCKv1.

213 Pairing LAMP with CRISPR/Cas12b enabled these assays to overcome non-specific
214 signal that can occur in assays using LAMP alone. In the SHERLOCKv2 assays, stochastic non-
215 specific LAMP products did not lead to Cas cleavage signal. Although isothermal amplification-
216 based methods recently developed for aquaculture diagnostics have shown that sequence-specific
217 probes can enhance assay specificity (28, 29), the combination of primers and probes cannot
218 always be relied on for sequence-specific detection (30). Cas detection systems rely on sequence-
219 specific target binding to induce conformational change that triggers cleavage activity (31), and
220 combining isothermal amplification methods with this additional layer of specificity is becoming
221 more common in aquaculture molecular diagnostic approaches (23, 32). Despite reports of single

222 insertion and deletion tolerance in some Cas complexes (33), we found Cas12b to be highly
223 specific, supportive of previous reports of Cas12b specificity down to the single nucleotide level
224 (34).

225 Although disease diagnosis typically only requires a binary result, the ability to quantify
226 viral load can be useful. The significant correlations we found between SHERLOCKv2 assays
227 and qPCR assays suggest SHERLOCKv2 can be semi-quantitative. The TSV SHERLOCKv2
228 assay tended to underestimate viral copies relative to qPCR while the WSSV SHERLOCKv2
229 assay mostly showed similar viral copies to qPCR. These discrepancies could be explained by
230 differences in amplification efficiencies of different genomic target sequences. The TSV qPCR
231 assay targets near the beginning of the ORF1 (TSVgp1) region whereas the TSV SHERLOCK
232 assay targets near the end of the ORF2 region. The primers used for the OIE-recommended
233 WSSV qPCR protocol were designed to target a genomic region ~20 kb upstream of the VP28
234 gene region, while the LAMP primers and guide RNA for the WSSV SHERLOCK assay target
235 within the VP28 gene region itself. As amplification efficiency is affected by differences in
236 structure and sequence length in target regions as well as primers, it can be expected that
237 quantifications would differ between methods targeting different regions. Additionally, the
238 structural differences in the synthetic target standards used in the SHERLOCK assays (200-300
239 DNA or RNA fragments) and qPCR assays (plasmids) could have contributed to discrepancies in
240 results (35). Differences in data analysis between qPCR and SHERLOCKv2 methods could have
241 also contributed to discrepancies in viral detection among the infected shrimp samples. Samples
242 assessed in the qPCR assays were run in triplicate and required 2 of 3 replicates to have a Ct
243 value ≤ 40 for diagnosis, while samples assessed in the SHERLOCKv2 assays more strictly
244 required 3 of 5 replicates pass a baseline and an outlier threshold. Despite the differences in

245 analysis methods and in the nature of template used to optimize the SHERLOCK assay
246 compared to the qPCR assay, the binary qualitative results in detecting virus in shrimp tissue
247 showed positive percent agreements (87% for TSV SHERLOCKv2 and 94% for WSSV
248 SHERLOCKv2) and negative percent agreements (100% for both assays) within or close to the
249 strict range required by the FDA for clinical SARS-CoV-2 assays (90% positive percent
250 agreement and 95% negative percent agreement) (36). Moreover, the quantitative loads of the
251 corresponding viruses as measured by the two assays were also comparable. This gives validity
252 to the SHERLOCKv2 assays when compared to the current gold standard of TSV and WSSV
253 detection recommended by the OIE.

254 With molecular diagnostics rapidly advancing alongside outbreaks of existing and
255 emerging disease, the transfer of technology from human diagnostics to animal fields is critical,
256 particularly to those that support global food security. With a growing need to support
257 aquaculture production, we demonstrated the ability to adapt a SHERLOCK assay developed for
258 human diagnostics for detecting RNA and DNA shrimp pathogens. This development of novel (±
259 RT)-LAMP + CRISPR/Cas diagnostic assays for TSV and WSSV monitoring in *P. vannamei*
260 and potential for field-deployable conversion will accelerate biomonitoring for shrimp
261 aquaculture and pave the way for the developing rapid, efficient diagnostics across the
262 agriculture field.

263 **METHODS**

264 *Viral challenge experiments*

265 For TSV, two independent challenge experiments were conducted using *P. vannamei*
266 lines that differ in TSV susceptibility and TSV isolates that differ in virulence. The purpose of
267 this was to generate tissues with a wide dynamic range of viral load. In one experiment, TSV-

268 susceptible specific pathogen free (SPF) *P. vannamei* shrimp (Kona line) were injected with TSV
269 inoculum (El Salvador isolate) intramuscularly and reared until animals were moribund. In a
270 second experiment, individuals from a commercial line of TSV-tolerant *P. vannamei* were
271 injected with a TSV inoculum (Belize isolate) intramuscularly. Shrimp tissues were preserved in
272 Davidson's AFA fixative after which they were embedded, sectioned, stained with hematoxylin
273 and eosin, and examined under a light microscope. Histopathological evaluations were
274 performed using a subset of samples from the experimentally infected tolerant *P. vannamei* (N =
275 6) and susceptible *P. vannamei* (N = 5). The severity of the TSV infection was graded based on a
276 semi-quantitative scale ranging from Grade 0 to Grade 4: Grade 0 showing no signs of infection;
277 Grade 1 showing signs of infection by the pathogen but at levels that may be below those needed
278 for clinical disease classification; Grade 2 showing moderate signs of infection based on the
279 number and severity of pathogen-caused lesions; Grade 3 showing moderate to high signs of
280 infection based on the number and severity of pathogen-caused lesions; and Grade 4 showing
281 high signs of infection based on a high number of pathogen-caused lesions and tissue destruction
282 (37). Total RNA from experimentally TSV-challenged shrimp (N = 35) was extracted with the
283 Total RNA Purification Kit (NORGEN BIOTEK CORP) following the manufacturer's
284 recommendations. Quality and quantity were assessed using a NanoDrop™ (Thermo Fisher).
285 The RNA concentrations of all samples were normalized to approximately 30 ng μl^{-1} and TSV
286 was detected and quantified using a TaqMan™ Fast Virus 1-Step Master Mix (Applied
287 Biosystems™) following the OIE recommended protocol (38). All samples were run in triplicate
288 alongside plasmid standards with known copy numbers (100 - 1,000,000 copies). TSV load in
289 the experimentally challenged shrimp was calculated by extrapolating Ct values in the standard
290 curve generated using plasmid DNA template.

291 Unlike TSV, all commercially available *P. vannamei* lines are highly susceptible to
292 WSSV with shrimp mortality occurring 2-3 days post-challenge in routine bioassays conducted
293 in the Aquaculture Pathology Laboratory at University of Arizona. Details of the viral challenge
294 experiment with WSSV of *P. vannamei* are reported in Sullivan et al. 2019 (23). Briefly, specific
295 pathogen free shrimp were challenged by feeding WSSV infected tissue, and infection was
296 confirmed in moribund animals by histology. Genomic DNA was extracted with DNeasy spin
297 kits (Qiagen), quantified using a NanoDrop™ (Thermo Fisher), and quantified by qPCR using
298 TaqMan Fast Virus 1-Step Master Mix run on an ABI StepOne Plus system and following the
299 OIE protocol (39).

300 *TSV and WSSV SHERLOCK assay development*

301 To identify genomic targets for TSV and WSSV viral detection, publicly available viral
302 genome sequences were searched for consensus regions. For TSV, eight genomes were retrieved
303 from GenBank (https://www.ncbi.nlm.nih.gov/genbank/; JF966384.1 (40), NC_003005.1 (41),
304 JX094350.1 (42), AF277675.1 (43), GQ502201.1 (44), DQ104696.1 (45), AY997025.1 (46),
305 DQ212790.1 (47)) and aligned with MAFFT (48) using the default parameters to generate a
306 consensus sequence (**Table S1**). For WSSV, the highly conserved viral envelope protein 28 (49)
307 was selected as a target and conservation across multiple strains was confirmed by surveying a
308 consensus genome compiled from 10 different isolates as previously reported (23).

309 To generate candidate LAMP primer sets, target sequences were input into the NEB
310 LAMP Primer Design tool (https://lamp.neb.com). For TSV, three LAMP primer sets were
311 selected as well as a previously published LAMP primer set (24) for screening. For WSSV, four
312 different candidate LAMP primer sets were selected and the primer set was optimized by testing
313 sets containing different combinations of primers as well as primer modifications including the

314 addition of a poly-T linker between the F1c/B1c and F2/B2 annealing sites of the FIP and BIP
315 primers (**Table S1**).
316 Guide RNAs for Cas12b collateral cleavage were designed using a sliding window of 20
317 bases in length and advancing one base at a time across the region between the F2 and B2
318 annealing sites of the LAMP FIP and BIP primers. To synthesize guide RNAs, a gBlock™
319 containing the *Aap* Cas12b sgRNA scaffold sequence (IDT) was first amplified using a forward
320 primer containing the T7 promoter sequence and reverse primers containing each different spacer
321 sequence. Amplification reaction conditions were as follows: 1X HF Buffer (NEB), 200 µM
322 dNTPs (NEB), 0.5 µM forward primer, 0.5 µM reverse primer, 0.01 ng template DNA, and 1
323 unit Phusion DNA polymerase (NEB) in 50 µL. Reactions were run on a thermocycler (Applied
324 Biosystems) with the following parameters: 98°C for 2 minutes, 30 cycles of 98°C for 10
325 seconds, 58°C for 30 seconds, and 72°C for 15 seconds, 72°C for 5 minutes, and a hold at 10°C.
326 Products were gel purified using the QIAquick Gel Extraction kit (Qiagen) with a 2% agarose 1x
327 TAE gel and products were eluted in 30 µL of Buffer EB prewarmed to 50°C. Concentrations
328 were measured using the Qubit Broad Range dsDNA kit (Life Technologies). Next, *in vitro*
329 transcription reactions were performed using the Ampliscribe T7 flash transcription kit (Lucigen)
330 in a 40 µL reaction with 50 ng of DNA template, 9 mM of each ribonucleotide, 9 mM of DTT, 1
331 µL of RiboGuard RNase inhibitor, 4 µL of T7 RNA polymerase, and 1X transcription reaction
332 buffer. Reactions were run at 42°C for 4 hours, incubated with 2 µL of DNase I (Lucigen) at
333 37°C for 15 minutes, and purified using the RNA Clean and Concentrate Kit (Zymo Research).
334 Guide RNAs were quantified using the Qubit Broad Range RNA assay kit (Life Technologies)
335 and molarity was estimated using the NEB copy number converter

336 (https://nebiocalculator.neb.com/). All sequences from the consensus genome, gBlocks™,
337 primers, and guide RNAs are listed in **Table S1**.

338 *Evaluating LAMP primers*

339 For TSV, primer sets were screened against a synthetic TSV RNA target *in vitro*
340 transcribed from gBlock™ DNA (IDT, **Table S1**) using the Ampliscribe T7-Flash Transcription
341 kit (Lucigen Corporation) and purified using the RNA Clean and Concentrator kit (Zymo
342 Research) following manufacturer's instructions. For WSSV, primer sets were screened against
343 either a synthetic WSSV DNA target (gBlock™, IDT; **Table S1**) or genomic DNA isolated from
344 shrimp with a high WSSV load. Target nucleic acid was diluted in background nucleic acid from
345 SPF shrimp as detailed in **Table S2** to improve the specificity of the LAMP primers. Total RNA
346 from SPF shrimp was isolated using the RNeasy blood and tissue kit (Qiagen) and genomic
347 DNA from SPF shrimp was isolated using the DNeasy blood and tissue kit (Qiagen). LAMP
348 reactions were prepared as detailed in **Table S2** and run at 60°C and 62°C (TSV and WSSV;
349 respectively) for 1 hour on a thermocycler for real-time PCR (QuantStudio 12K flex, Thermo
350 Fisher) with fluorescent measurements taken at 2-minute intervals. Successful primers were
351 determined by their ability to start amplification before 30 minutes.

352 *Evaluating guide RNAs and Cas12b detection*

353 Guide RNAs were systematically evaluated with Recombinant *Aap* Cas12b (GenScript)
354 for efficacy using TSV LAMP product or synthetic WSSV target DNA (gBlock™, IDT) in 20
355 µL (TSV) or 10 µL (WSSV) reactions described **Table S2**. Prior to adding template and reporter,
356 reaction mixtures were incubated for 15 minutes at room temperature to facilitate the formation
357 of the CRISPR/Cas ribonucleoprotein complex. For each guide RNA, a negative control was run
358 that did not contain target nucleic acid to measure background collateral cleavage, and all

359 reactions were run in triplicate. Reactions were run in a 384-well black clear bottom plate
360 (Corning) at 60°C for 1 hour with measurements recorded every 2 minutes using a Spectramax
361 iD3 plate reader (Molecular Devices). Effective guide RNAs were identified as those that
362 generate a signal well-distinguished from the negative control in less than 30 minutes.

363 *Evaluating sensitivity and standard curve generation*

364 To produce standard curves for each assay, one-pot LAMP-Cas12b SHERLOCK
365 reactions were run using either *in vitro* transcribed synthetic TSV RNA target, synthetic WSSV
366 DNA target (gBlock™, IDT; **Table S1**), or genomic DNA isolated from shrimp with a high viral
367 load. Ten-fold dilution series of synthetic DNA or RNA were made ranging from 10^1 to 10^6
368 copies μL^{-1} (TSV) or 10^1 to 10^{10} copies μL^{-1} (WSSV) with all samples diluted in specific
369 pathogen free shrimp genomic RNA (5 ng per 20 µL reaction for TSV) or DNA (20 ng per 20
370 µL reaction for WSSV). Negative control reactions that did not contain any target nucleic acid
371 were included in each experiment. Reactions were run with 5 replicates per sample prepared as
372 detailed in **Table S2** and run at 60°C (TSV) or 62°C (WSSV) using a QuantStudio 12k Flex
373 thermocycler for real-time PCR (Applied Biosystems) for 60 minutes, with fluorescence readings
374 every 2 minutes. Prior to adding dNTPs, Bst, primer mix, fluorescent reporter, SYTO-82 dye, or
375 DNA, other reaction components were combined and incubated for 15 minutes at room
376 temperature to facilitate the formation of the CRISPR/Cas ribonucleoprotein complex.

377 *Evaluating SHERLOCK quantification*

378 To compare quantification of viral loads estimated by the OIE-recommended qPCR and
379 SHERLOCK, one-pot TSV SHERLOCK reactions were run on the same RNA samples from 30
380 TSV-infected shrimp quantified by qPCR described above. For WSSV, one-pot SHERLOCK
381 reactions were run on the same DNA samples from 35 WSSV-infected shrimp previously

382 quantified by qPCR (23). To standardize input across samples, 10 ng of RNA (TSV) or 1 ng of
383 DNA (WSSV) was added per 20 µL SHERLOCK reaction. SHERLOCK reactions were
384 prepared as detailed in **Table S2**, and all samples were run alongside standard curves as
385 described above. A linear regression analysis was performed on Ct values from the standard
386 curve samples calculated from fluorescent measurements that were corrected to a baseline
387 defined by cycles 1-2 for WSSV and 1-4 for TSV, and viral copies were estimated for each
388 sample from the extrapolated standard Ct values. For each sample, including standards, any
389 replicate outlier based on a Ct value beyond the sample median Ct ± one cycle was excluded and
390 only samples with at least three out of five replicates were considered in downstream analyses.
391 Viral copies estimated by SHERLOCK one-pot reactions were then compared to those estimated
392 by qPCR using a Pearson correlation analysis.

393 *Evaluating specificity*

394 The specificity of each one-pot SHERLOCK assay was tested against either RNA or
395 DNA extracted from shrimp tissue infected with infectious myonecrosis virus (IMNV; muscle
396 tissue), infectious hypodermal and haematopoietic necrosis virus (IHHNV; muscle tissue), *V.*
397 *parahaemolyticus* causing acute hepatopancreatic necrosis disease/early mortality syndrome
398 (AHPND/EMS; hepatopancreas tissue), and *Enterocytozoon hepatopenaei* (EHP; hepatopancreas
399 tissue). RNA was extracted using RNeasy mini plus kit (Qiagen) and DNA was extracted using
400 the Qiagen DNeasy blood and tissue kit following manufacturer's protocols. One-pot reactions
401 were prepared as detailed in **Table S2** with a total of 10 ng of sample RNA (TSV) or 1 ng of
402 sample DNA (WSSV) in each reaction. To estimate false positive rates, one-pot reactions were
403 prepared as detailed in **Table S2** and run as described above with 5 ng of total RNA or 20 ng of
404 genomic DNA isolated from muscle tissue from 10 individual specific pathogen-free shrimp.

405 *Data availability*

406 Raw fluorescence data from all qPCR and SHERLOCK experiments, and R code used to

407 generate plots and statistics is publicly available at https://doi.org/10.5281/zenodo.7438263 (50).

408

409 **ACKNOWLEDGEMENTS**

410 We thank Veronica L. Pereira and Zachary G. Dench (Gloucester Marine Genomics Institute) for
411 their contributions towards previous iterations of assay development that inspired the assay
412 design described here. We also thank New England BioLabs and Sherlock Biosciences for
413 helpful discussions and advice.

414

415 **FUNDING**

416 This work was supported by the United States Department of Agriculture NIFA AFRI
417 Exploratory Research Program (grant # 2018-08980)

418

419 **AUTHOR CONTRIBUTIONS**

420 S.R.M. and S.A.T. designed and performed molecular experiments, analyzed the data, and wrote
421 the manuscript; M.J.H provided input throughout the project and edited the manuscript; R.C.-F.
422 conducted histopathology and preliminary qPCR experiments; A.K.D. provided all laboratory
423 challenge samples, developed the experimental design, managed the histopathology verification,
424 provided input throughout the project, and contributed to manuscript revisions; A.G.B.
425 conceived the project, provided input throughout its progress, and edited the manuscript.

426

427 **REFERENCES**

428 1. Cammilleri G, Ferrantelli V, Pulvirenti A, Drago C, Stampone G, del Rocio Quintero
429 Macias G, Drago S, Arcoleo G, Costa A, Geraci F, di Bella C. 2020. Validation of a
430 Commercial Loop-Mediated Isothermal Amplification (LAMP) Assay for the Rapid
431 Detection of Anisakis spp. DNA in Processed Fish Products. Foods 9.

2. Gootenberg JS, Abudayyeh OO, Lee JW, Essletzbichler P, Dy AJ, Joung J, Verdine V, Donghia N, Daringer NM, Freije CA, Myhrvold C, Bhattacharyya RP, Livny J, Regev A, Koonin E v., Hung DT, Sabeti PC, Collins JJ, Zhang F. 2017. Nucleic acid detection with CRISPR-Cas13a/C2c2. Science (1979) 356:438–442.

3. de Puig H, Lee RA, Najjar D, Tan X, Soekensen LR, Angenent-Mari NM, Donghia NM, Weckman NE, Ory A, Ng CF, Nguyen PQ, Mao AS, Ferrante TC, Lansberry G, Sallum H, Niemi J, Collins JJ. 2021. Minimally instrumented SHERLOCK (miSHERLOCK) for CRISPR-based point-of-care diagnosis of SARS-CoV-2 and emerging variants. Sci Adv 7.

4. Joung J, Ladha A, Saito M, Kim N-G, Woolley AE, Segel M, Barretto RPJ, Ranu A, Macrae RK, Faure G, Ioannidi EI, Krajeski RN, Bruneau R, Huang M-LW, Yu XG, Li JZ, Walker BD, Hung DT, Greninger AL, Jerome KR, Gootenberg JS, Abudayyeh OO, Zhang F. 2020. Detection of SARS-CoV-2 with SHERLOCK one-pot testing. N Engl J Med 383:1492–1494.

5. FAO. 2020. The State of World Fisheries and Aquaculture 2020. Sustainability in action. 1–244.

6. Naylor RL, Kishore A, Sumaila UR, Issifu I, Hunter BP, Belton B, Bush SR, Cao L, Gelcich S, Gephart JA, Golden CD, Jonell M, Koehn JZ, Little DC, Thilsted SH, Tigchelaar M, Crona B. 2021. Blue food demand across geographic and temporal scales. Nat Commun 12:1–14.

7. Stentiford GD, Neil DM, Peeler EJ, Shields JD, Small HJ, Flegel TW, Vlak JM, Jones B, Morado F, Moss S, others. 2012. Disease will limit future food supply from the global crustacean fishery and aquaculture sectors. J Invertebr Pathol 110:141–157.

454 8. National Marine Fisheries Service. 2022. Fisheries of the United States, 2020. US
455 Department of Commerce, NOAA Current Fishery Statistics No. 2020.

456 9. Lafferty KD, Harvell CD, Conrad JM, Friedman CS, Kent ML, Kuris AM, Powell EN,
457 Rondeau D, Saksida SM. 2015. Infectious diseases affect marine fisheries and aquaculture
458 economics. Ann Rev Mar Sci 7:471–496.

459 10. Hasson KW, Lightner D V, Mohney LL, Redman RM, Poulos BT, White BM. 1999.
460 Taura syndrome virus (TSV) lesion development and the disease cycle in the Pacific white
461 shrimp *Penaeus vannamei*. Dis Aquat Organ 36:81–93.

462 11. Zhan W-B, Wang Y-H, Fryer JL, Yu K-K, Fukuda H, Meng Q-X. 1998. White spot
463 syndrome virus infection of cultured shrimp in China. J Aquat Anim Health 10:405–410.

464 12. Brock JA. 1997. Taura syndrome, a disease important to shrimp farms in the Americas.
465 World J Microbiol Biotechnol 13:415–418.

466 13. Lightner D v., Redman RM, Pantoja CR, Tang KFJ, Noble BL, Schofield P, Mohney LL,
467 Nunan LM, Navarro SA. 2012. Historic emergence, impact and current status of shrimp
468 pathogens in the Americas. J Invertebr Pathol 110:174–183.

469 14. Tu C, Huang H-T, Chuang S-H, Hsu J-P, Kuo S-T, Li N-J, Hsu T-L, Li M-C, Lin S-Y.
470 1999. Taura syndrome in Pacific white shrimp *Penaeus vannamei* cultured in Taiwan. Dis
471 Aquat Organ 38:159–161.

472 15. Argue BJ, Arce SM, Lotz JM, Moss SM. 2002. Selective breeding of Pacific white shrimp
473 (*Litopenaeus vannamei*) for growth and resistance to Taura Syndrome Virus. Aquaculture
474 204:447–460.

475 16. Lillehammer M, Bangera R, Salazar M, Vela S, Erazo EC, Suarez A, Cock J, Rye M,
476 Robinson NA. 2020. Genomic selection for white spot syndrome virus resistance in
477 whiteleg shrimp boosts survival under an experimental challenge test. Sci Rep 10.

478 17. Eswaran S. 2021. Specific Pathogen Free (SPF) Shrimps in Aquaculture, p. 465–470. *In*
479 Pandey, P, Parhi, J (eds.), Advances in Fisheries Biotechnology. Springer, Singapore.

480 18. Sivakumar S, Vimal S, Abdul Majeed S, Santhosh Kumar S, Taju G, Madan N, Rajkumar
481 T, Thamizhvanan S, Shamsudheen K v., Scaria V, Sivasubbu S, Sahul Hameed AS. 2018.
482 A new strain of white spot syndrome virus affecting *Litopenaeus vannamei* in Indian
483 shrimp farms. J Fish Dis 41:1129–1146.

484 19. Restrepo L, Reyes A, Bajaña L, Betancourt I, Bayot B. 2018. Draft genome sequence of a
485 White Spot Syndrome Virus isolate obtained in Ecuador. Genome Announc 6.

486 20. Oakey HJ, Smith CS. 2018. Complete genome sequence of a white spot syndrome virus
487 associated with a disease incursion in Australia. Aquaculture 484:152–159.

488 21. Jacobson RH, Wright P. 2022. Principles and methods of validation of diagnostic assays
489 for infectious diseases, p. 11–26. *In* Manual of Diagnostic Tests for Aquatic Animals.
490 World Organization of Animal Health (Office International des Epizooties).

491 22. Flegel TW. 2019. A future vision for disease control in shrimp aquaculture. J World
492 Aquac Soc 50:249–266.

493 23. Sullivan TJ, Dhar AK, Cruz-Flores R, Bodnar AG. 2019. Rapid, CRISPR-based, field-
494 deployable detection of White Spot Syndrome Virus in shrimp. Sci Rep 9:1–7.

495 24. Kiatpathomchai W, Jareonram W, Jitrapakdee S, Flegel TW. 2007. Rapid and sensitive
496 detection of Taura syndrome virus by reverse transcription loop-mediated isothermal
497 amplification. J Virol Methods 146:125–128.

498 25. Wei S, Suryawanshi H, Djandji A, Kohl E, Morgan S, Hod EA, Whittier S, Roth K, Yeh
499 R, Alejaldre JC, Fleck E, Ferrara S, Hercz D, Andrews D, Lee L, Hendershot KA,
500 Goldstein J, Suh Y, Mansukhani M, Williams Z. 2021. Field-deployable, rapid diagnostic
501 testing of saliva for SARS-CoV-2. Sci Rep 11:1–9.

502 26. Tang-Nelson F-J, Lo C-F. 2021. Manual of Diagnostic Tests for Aquatic Animals 2021,
503 8th ed. World Organization of Animal Health (Office International des Epizooties).
504 Retrieved 22 June 2022.

505 27. Srisuvan T, Noble BL, Schofield PJ, Lightner D v. 2006. Comparison of four Taura
506 syndrome virus (TSV) isolates in oral challenge studies with *Litopenaeus vannamei*
507 unselected or selected for resistance to TSV. Dis Aquat Organ 71:1–10.

508 28. Zhang T, Liu X, Yang X, Liu F, Yang H, Li X, Feng H, Wu X, Jiang G, Shen H, Dong J.
509 2022. Rapid on-site detection method for White Spot Syndrome Virus using Recombinase
510 Polymerase Amplification combined with lateral flow test strip technology. Front Cell
511 Infect Microbiol 12:1008.

512 29. Kampeera J, Dangtip S, Suvannakad R, Khumwan P, Senapin S, Kiatpathomchai W.
513 2021. Reverse transcription loop-mediated isothermal amplification (RT-LAMP)
514 combined with colorimetric gold nanoparticle (AuNP) probe assay for visual detection of
515 tilapia lake virus (TiLV) in Nile and red hybrid tilapia. J Fish Dis 44.

516 30. Hardinge P, Murray JAH. 2019. Lack of specificity associated with using molecular
517 beacons in loop mediated amplification assays. BMC Biotechnol 19.

518 31. Saha A, Arantes PR, Hsu R v., Narkhede YB, Jinek M, Palermo G. 2020. Molecular
519 dynamics reveals a DNA-induced dynamic switch triggering activation of CRISPR-
520 Cas12a. J Chem Inf Model 60.

521 32. Naranitus P, Aiamsa-at P, Sukonta T, Hannanta-anan P, Chaijarasphong T. 2022.
522 Smartphone-compatible, CRISPR-based platforms for sensitive detection of acute
523 hepatopancreatic necrosis disease in shrimp. J Fish Dis 45:1805–1816.

524 33. Zhang W, Shi R, Dong K, Hu H, Shu W, Mu Y, Yan B, Li L, Xiao X, Wang H. 2022. The
525 off-target effect of CRISPR-Cas12a system toward insertions and deletions between target
526 DNA and crRNA sequences. Anal Chem 94:8596–8604.

527 34. Teng F, Guo L, Cui T, Wang XG, Xu K, Gao Q, Zhou Q, Li W. 2019. CDetection:
528 CRISPR-Cas12b-based DNA detection with sub-attomolar sensitivity and single-base
529 specificity. Genome Biol 20:132.

530 35. Bowers RM, Dhar AK. 2011. Effect of template on generating a standard curve for
531 absolute quantification of an RNA virus by real-time reverse transcriptase-polymerase
532 chain reaction. Mol Cell Probes 25:60–64.

533 36. Brooks ZC, Das S. 2020. COVID-19 testing impact of prevalence, sensitivity, and
534 specificity on patient risk and cost. Am J Clin Pathol 154:575–584.

535 37. Lightner DV (ed.). 1996. A handbook of shrimp pathology and diagnostic procedures for
536 diseases of cultured penaeid shrimp. Baton Rouge, LA (USA) World Aquaculture Society.

537 38. Tang KFJ, Wang J, Lightner D V. 2004. Quantitation of Taura syndrome virus by real-
538 time RT-PCR with a TaqMan assay. J Virol Methods 115:109–114.

539 39. Durand S v., Lightner D v. 2002. Quantitative real time PCR for the measurement of
540 white spot syndrome virus in shrimp. J Fish Dis 25:381–389.

541 40. Aranguren LF, Salazar M, Tang K, Caraballo X, Lightner D. 2013. Characterization of a
542 new strain of Taura syndrome virus (TSV) from Colombian shrimp farms and the
543 implication in the selection of TSV resistant lines. J Invertebr Pathol 112:68–73.

544 41. Mari J, Poulos BT, Lightner D v., Bonami JR. 2002. Shrimp Taura syndrome virus:
545 genomic characterization and similarity with members of the genus Cricket paralysis-like
546 viruses. J Gen Virol 83:915–926.

547 42. Tang KFJ, Navarro SA, Pantoja CR, Aranguren FL, Lightner D v. 2012. New genotypes
548 of white spot syndrome virus (WSSV) and Taura syndrome virus (TSV) from the
549 Kingdom of Saudi Arabia. Dis Aquat Organ 99:179–185.

550 43. Mari J, Poulos BT, Lightner D v., Bonami JR. 2002. Shrimp Taura syndrome virus:
551 genomic characterization and similarity with members of the genus Cricket paralysis-like
552 viruses. J Gen Virol 83:915–926.

553 44. Dhar AK, Lakshman DK, Amundsen K, Robles-Sikisaka R, Kaizer KN, Roy S, Hasson
554 KW, Allnutt FCT. 2010. Characterization of a Taura syndrome virus isolate originating
555 from the 2004 Texas epizootic in cultured shrimp. Arch Virol 155:315–327.

556 45. Huang XX, Lu CP. 2005. The molecular diagnosis and phylogenetic analysis of Taura
557 Syndrome Virus isolated in China. https://www.ncbi.nlm.nih.gov/nuccore/DQ104696.1.

558 46. Srisuvan T, Tang KFJ, Lightner D v. 2005. Experimental infection of *Penaeus monodon*
559 with Taura syndrome virus (TSV). Dis Aquat Organ 67:1–8.

560 47. Côté I, Navarro S, Tang KFJ, Noble B, Lightner D v. 2008. Taura syndrome virus from
561 Venezuela is a new genetic variant. Aquaculture 284:62–67.

562 48. Katoh K, Misawa K, Kuma KI, Miyata T. 2002. MAFFT: a novel method for rapid
563 multiple sequence alignment based on fast Fourier transform. Nucleic Acids Res 30:3059–
564 3066.

565 49. You Z, Nadala ECB, Yang J, Loh PC. 2004. Conservation of the DNA sequences
566 encoding the major structural viral proteins of WSSV. Dis Aquat Organ 61:159–163.

567 50. Trigg SA. 2022. shellytrigg/paper-TSV_WSSV_SHERLOCKv2: TSV-WSSV-
568 SHERLOCKv2_ms (v5.0). Zenodo. https://doi.org/10.5281/zenodo.7438263.

569
570

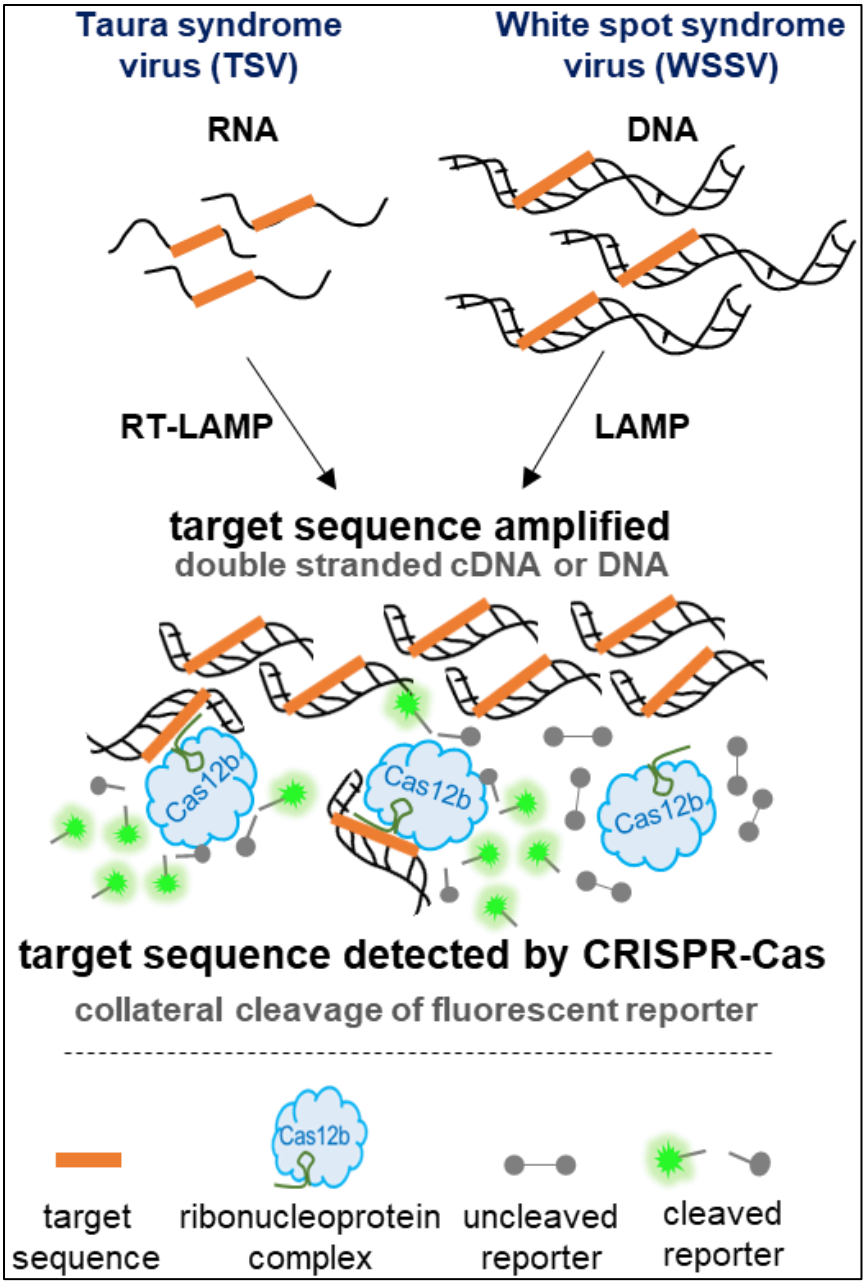

571
572

573 **Figure 1.** Schematic for CRISPR-based DNA and RNA detection in a one-pot reaction with

574 simultaneous isothermal amplification of target sequence and detection by CRISPR-Cas target

575 binding and collateral cleavage of a fluorescent reporter.

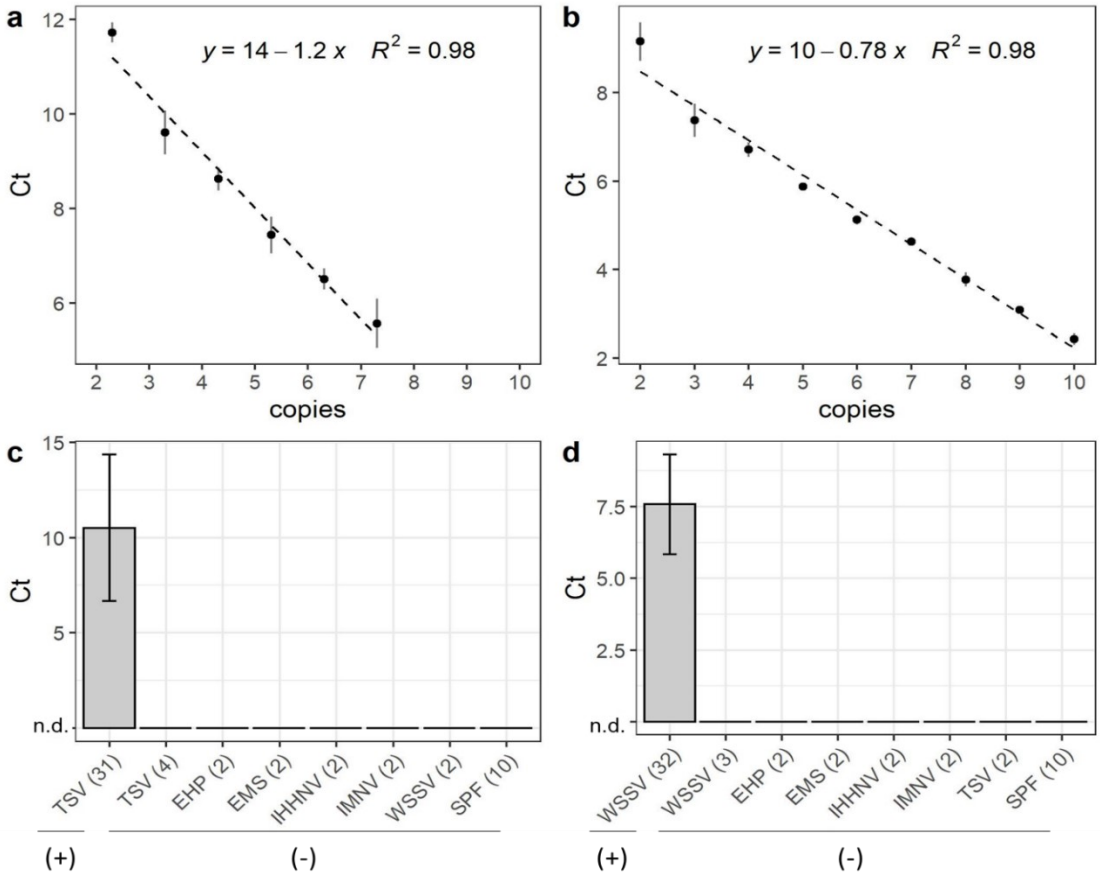

576

577 **Figure 2.** Sensitivity and specificity of SHERLOCK assays. SHERLOCK assay 10-fold standard

578 curve showing Ct values (mean +/- s.d. of five technical replicates) for synthetic (**a**) TSV RNA

579 and (**b**) WSSV DNA target with the dashed line indicating linear regression. Ct values (mean +/-

580 s.d).; n.d., not detected) from SHERLOCK specificity tests evaluating shrimp samples for the

581 detection of (**c**) TSV and (**d**) WSSV against other common white shrimp diseases including

582 Vibrio spp. (causing EMS), EHP, IHHNV, IMNV, and pathogen-free shrimp (SPF). (+) and (-)

583 indicate assay results.

584

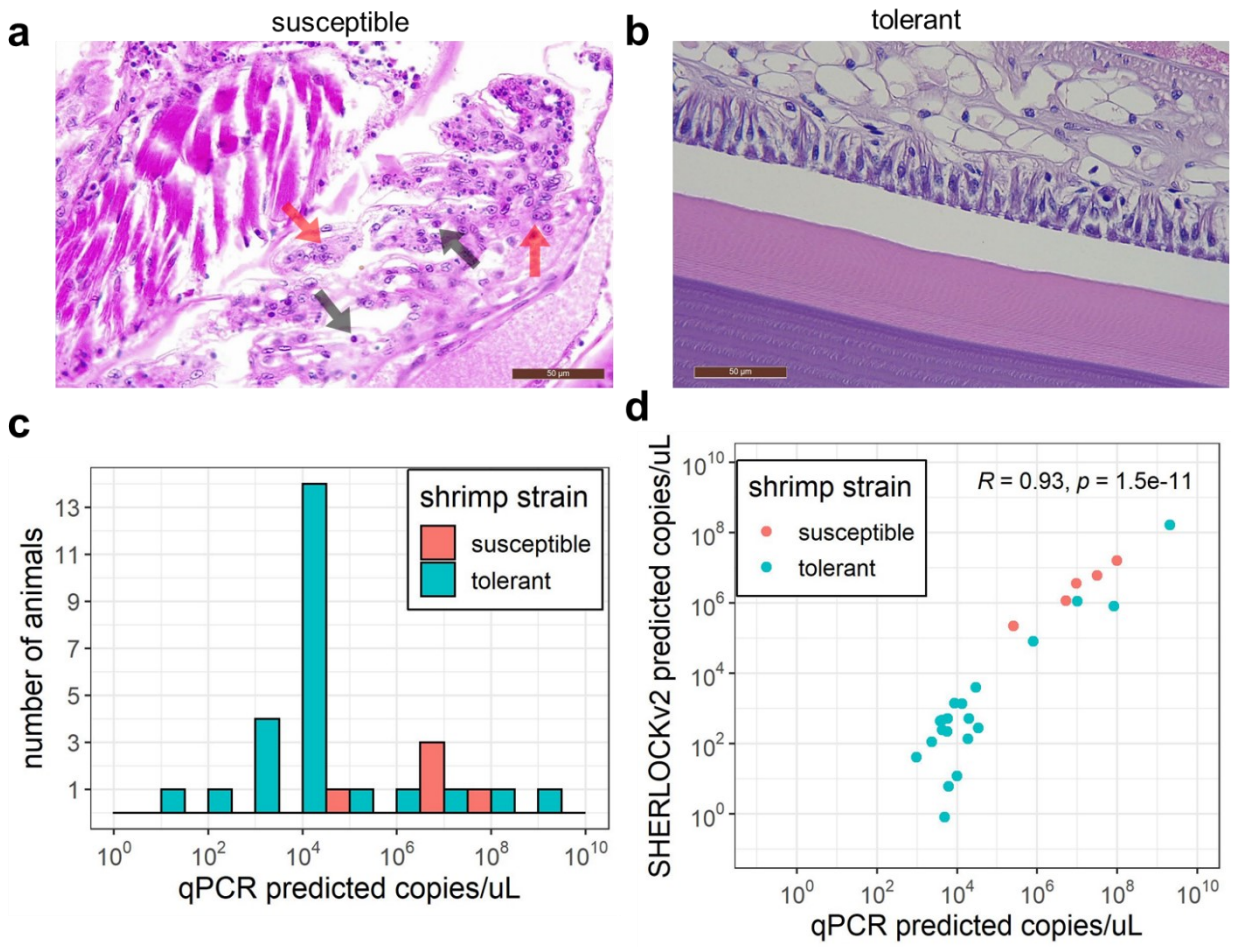

Figure 3. TSV SHERLOCK validation. (**a**) H & E-stained representative section from *P. vannamei* susceptible line after TSV exposure showing focal acute-phase infection in the gill characterized by spherical intracytoplasmic inclusions bodies (black arrows), pyknosis (red arrows) and karyorrhexis. (**b**) H & E-stained representative section from *P. vannamei* resistant line after TSV exposure showing no pathological signs characteristic of TSV infection. (**c**) TSV load quantified by qPCR in resistant (coral) and susceptible animals (teal). (**d**) Correlation between qPCR and TSV SHERLOCK quantification.

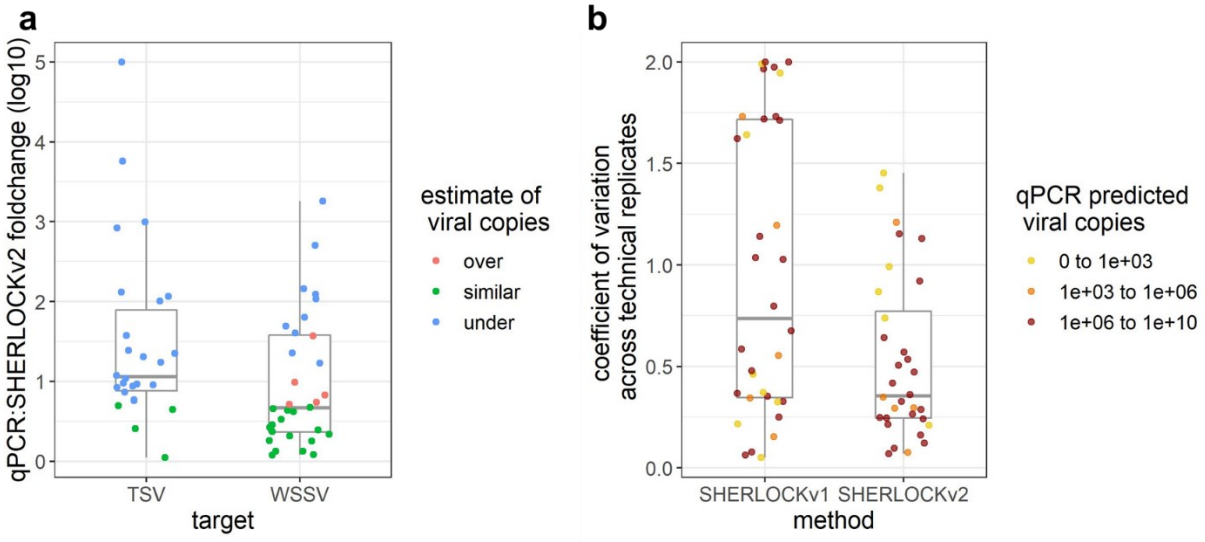

Figure 4. Comparison of SHERLOCKv2 assays to existing molecular assays. (**a**) Fold change in viral copies estimated by SHERLOCKv2 assays relative to qPCR assays for commonly tested samples. (**b**) Variation across technical replicates for WSSV samples commonly assayed in SHERLOCKv1 and SHERLOCK v2 assays.

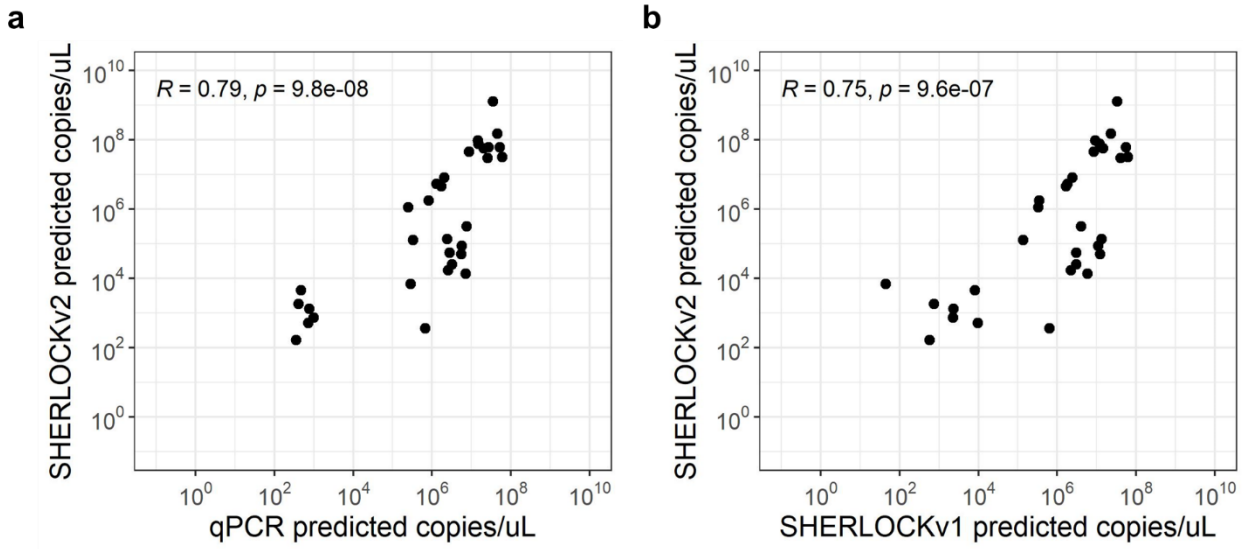

Figure 5. WSSV SHERLOCK assay validation. (**a**) Correlation between qPCR and WSSV SHERLOCKv2 assay quantification (error bars, +/- s.d.). (**b**) Correlation between WSSV SHERLOCKv2 and WSSV SHERLOCKv1 assays.